TECHNICAL MEMORANDUMS

NATIONAL ADVISORY COMMITTEE FOR AERONAUTICS

No. 990

CONTRIBUTION TO THE AERODYNAMICS OF ROTATING-WING AIRCRAFT

PART II

By G. Sissingh

Luftfahrtforschung
Vol. 17, No. 7, July 20, 1940
Verlag von R. Oldenbourg, München und Berlin

Washington
October 1941

NATIONAL ADVISORY COMMITTEE FOR AERONAUTICS

TECHNICAL MEMORANDUM NO. 990

CONTRIBUTION TO THE AERODYNAMICS OF ROTATING-WING AIRCRAFT*

PART II

By G. Sissingh

The interrelations established in an earlier report on this subject (NACA T.M. No. 921) are used to study the best assumptions for hovering and horizontal flight. The effect of the twisted and tapered blade on the rotor efficiency is analyzed and the gliding coefficient at different stages (from autogiro to helicopter) of horizontal flight compared. To the extent that model or full-scale test data are available, they are included in the comparison.

NOTATION

In addition to the notation employed in the earlier report (T.M. No. 921), the following symbols are used:

G (kg) tare weight of aircraft

N (hp) rotor input power

N_z (hp) input power of regular propeller on autogiro or helicogyro

ν factor identifying the flight stage

$$\nu = \frac{N}{N + N_z}$$

$\nu = 0$ autogiro

$\nu = 1$ helicopter

$1 > \nu > 0$ helicogyro

*"Beitrag zur Aerodynamik der Drehflügelflugzeuge, Part II, Luftfahrtforschung, vol. 17, no. 7, July 20, 1940, pp. 196-203. (Part I has been published as NACA T.M. No. 921.)

η static-thrust efficiency: $\eta = \frac{k_{sa}^{3/2}}{2k_d} = M - .707 \frac{C_T^{3/2}}{C_Q}$

ϵ gliding coefficient of rotating-wing aircraft, rotor-gear efficiency, and efficiency of normal propeller equated to 1:

$$\epsilon = \frac{k_{sh} + f \lambda^2}{k_{sv}} + \frac{k_d}{\lambda k_{sv}}$$

with $\lambda = V/U \cong \mu$

f ratio of parasite area of all nonlifting parts of the aircraft to swept rotor-disk area F

$\sigma_{0.7}$ reduced solidity of a tapered blade; σ referred to blade chord at 0.7R

$$\sigma_{0.7} = \frac{z\, t_0\, (1 + 0.7\, p)}{\pi R}$$

GENERALITIES

Depending upon the purpose of use of the rotating-wing aircraft as load carrier, where the speed is secondary, or as air liner with high cruising speed - the principal value is placed on a high rotor lifting power or a good lift/drag ratio of the aircraft. However, since one requirement of a rotating-wing aircraft is its ability to take off and land vertically, the tare weight and the rotor power available decide the minimum diameter of the rotor disk. Decisive, finally, is the thrust per unit power, which follows at

$$G/N = 75\, \eta \sqrt{\frac{2\rho}{G/F}} \quad \text{kg/hp} \qquad (78)$$

As regards the static-thrust efficiency, η, it suffices to state that, for the present, it ranges from 60 to 75 percent and depends upon the aerodynamic design of the rotor.

According to equation (78) and figure 8, the lift capacity of a rotor increases with decreasing blade loading which, for modern airplanes of from about 800 to

1000 kilograms total weight, ranges from 6 to 10 kg/m^2, and more for larger and faster types.

Figure 9 illustrates the relation between diameter, total weight, and power according to equation (78), at $\eta = 0.7$ static-thrust efficiency. The diameter resulting from figure 9 would just suffice to keep the aircraft hovering without ground effect.* Obviously, a certain excess lift is necessary for climbing, etc., which requires a correspondingly greater diameter. Solving equation (78) with respect to D, affords

$$D = 0.01065 \frac{G^{3/2}}{\eta N \sqrt{\rho}} \qquad (78a)$$

In other words, a desired percent of change of lift requires approximately 1.5 times the rotor diameter. At constant η, for instance, a 15-percent increase in diameter raises the lifting power 10 percent. But with consideration for the weight of the blades and the sag at static thrust**, this rotor enlargement cannot be continued arbitrarily.

Of further general importance is the circumferential speed at the tip circle, which on modern aircraft of the type Ar C 30 ranges from 100 to 150 meters per second and which - as shown later on - cannot be substantially changed for various reasons.

For estimated prediction of the best value, we quote the result of a subsequent calculation, which states that the best static thrust coefficient is secured by a blade loading of $k_{sa}/\sigma \cong 0.2$. With this value and D, according to equation (78a), the equation for the axial thrust ($G = k_{sa} F U^2 \frac{\rho}{2}$) gives as best tip speed in the hovering stage:

---

*In direct proximity of the ground, the thrust for equal power input is greater. This increase in lift is effective at a distance of 0.6 to 0.8 D between rotor disk and ground and can, for modern airplane types, amount to as much as 30 percent.

**To keep the blade stresses in flight to a minimum, they should be flexible in bending at right angles to the plane of rotation. In this manner, unloading from the centrifugal force makes it possible to lower the bending stress to about 20 percent of the inelastic blade.

$$U = \frac{335\ \eta\ N}{G\ \sqrt{\sigma}}\ m/s \qquad (79)$$

Figure 10 gives the tip speed plotted against the power loading conformable to equation (79) for the practical solidity ratios $\sigma = 0.04$ to 0.10. It is pointed out on this occasion that, while high σ favors the static-thrust coefficient, the lower σ is more propitious for horizontal flight. Figure 10 shows the power loading referred to the total weight. To enable the rotor to carry n times this total weight, the tip speed must further be reduced in the ratio 1:n. The thus-secured U value considers only the hovering stage or the climb. If, in addition, the airplane is to have high speed in level flight, other viewpoints are involved which restrict the range considerably.

Since the drag coefficient for normal profiles increases materially when operating in proximity of sonic velocity, high Mach numbers must be avoided as much as possible (reference 1). The highest relative speed on the rotating-wing aircraft is at the tip of the advancing blade ($\psi = 90^{\circ}$), where flight and circumferential speed become additive. If it is assumed that the sum of these two speeds is not permitted to exceed a specified value, the flying speed will be maximum for each circumferential speed.

Figure 11 illustrates this connection for different coefficients of advance λ (ratio of flight to circumferential speed). The limit following the requirement of a maximum permissible Mach number is included on the basis that the highest relative speed at the blade tip is not to exceed 90 percent of the velocity of sound. Since this high speed is confined to a small part of the rotor disk, the permissible Mach number might perhaps be raised a little without appreciable detriment to the gliding coefficient of the rotor. Theoretically, this produces no change in the speed limitation of rotating-wing aircraft.

Since the efficiency decisive for horizontal forward flight, the gliding coefficient (of the rotating-wing aircraft), reaches its best value by a coefficient of advance $\mu = 0.35$ to 0.40, the speed limit of the best horizontal flight is, according to figure 11, about 300 kilometers per hour. Of course, by foregoing the minimum gliding coefficient, it is quite possible to design rotating-

wing aircraft with speeds up to 400 kilometers per hour and more. The then-required coefficients of advance of 0.6 at around 180-meters-per-second tip speed are entirely within the realms of possibility.

However, it is pointed out, at this opportunity, that in the expressed high speed the performance of the rotating-wing aircraft is still likely always to be lower than that of the fixed-wing aircraft because of the high coefficients of advance connected with it. The chief advantage of the rotating-wing aircraft is that in spite of sufficient maximum speed, it is able to reduce its forward speed to the hovering stage. This quality will make it preferable to the orthodox airplane for many practical purposes, even if its top speed is lower.

DETERMINATION OF EFFICIENCIES

The calculation is based on the following substitute functions for the aerodynamic force coefficients of the blade element:

$$c_a = 5.6\ \alpha_p \tag{80}$$

$$c_w = 0.011 - 0.0572\ \alpha_p + 0.89\ \alpha_p^2 \tag{81}$$

These data approximately correspond to the U.S. airfoil M 12 at 1:30 aspect ratio. The parabola for c_w was chosen so that at $\alpha_p = 0^\circ$, 6.5°, and 13° the substitute function agrees with the true drag coefficient.*

The thrust-reduction factor B is - independent of the propeller loading and blade number - put at 0.98; that is, the outermost 2 percent of the rotor blade has no share in the lift. For simplicity, it is further assumed that

*Since the downwash is already contained in λ_d when determining the operating angles on the blade element - and moreover, the polar for finite aspect ratio is employed - the finite aspect ratio is allowed for, twice. The author chose this method intentionally, since it is the simplest way of obtaining agreement between theory and test. This method, though very useful, is therefore merely an expedient until acceptable downwash measurements and the polars of an airfoil under different angles of yaw make an exact calculation possible.

the flapping hinge coincides with the axis of rotation. The profile is the same as given in the earlier report (T.M. No. 921). The hub resistance is ignored for the present. The blade-mass constant on the rectangular blade is put at $\gamma = 12$. A tapered blade 3:1 ($p = -\frac{2}{3}$) of the same design which at 0.7R has the same chord as the rectangular version, has about $\gamma = 23.4$. This value was then used as the basis.

Static-Thrust Coefficient

For the hovering stage, the problem is to determine the assumptions for an optimum static-thrust coefficient:

$$\eta = \frac{k_{sa}^{3/2}}{2k_d} \tag{82}$$

First to be defined is the most beneficial (specific) blade loading k_{sa}/σ, which is an indication for an average operating angle on the blade element.* This calculation was made for an untwisted, rectangular blade by means of equations (11), (13), (14), and (82), and the data plotted against the blade loading in figure 12 for different thrust coefficients. The efficiency η rises with ascending thrust coefficient to a maximum at $k_{sa}/\sigma = 0.195$ blade loading, independent of k_{sa}.

The subsequent studies pertain to the improvement of the efficiency by suitable blade design. For this analysis, $k_{sa} = 0.009$ serves as a basis, which approximately corresponds to the thrust coefficient of modern rotating-wing aircraft.

Figure 13 shows the effect of twist on a rectangular blade, with solidity σ as abscissa instead of the blade loading. The best solidity in figure 13 is $\sigma \cong 5$ percent for $k_{sa} = 0.009$, which again corresponds to ~ 0.2 blade loading. It is also seen that a 12° twist raises the static thrust coefficient from 67.8 to 74.8 percent, or 10.3 percent over the blade with zero twist.

*For the rectangular blade, equation (13) affords for the average operating angle:

$$\alpha_p{}^\circ = \frac{3 \times 57.3}{c_a' B^3} k_{sa}/\sigma$$
$$\cong 32.6\ k_{sa}/\sigma$$

As a general rule, the rotor blades will have only a little twist in consideration of forward flight and the autorotation ability endangered by a greater twist. In practice, therefore, the twist is not likely to exceed 8° to 10°.

A further means for improving the static-thrust efficiency is afforded by the taper of the blade; that is, taper of blade chord toward the tip. Here also the improvement is the result of a more uniform spanwise load distribution, the resultant of the tangential forces governing the torque traveling inward and thus becoming effective on a shorter lever arm.

Figure 14 illustrates the improvement afforded by a change from a simple rectangular blade to the untwisted and twisted tapered blade. The best solidity is again reached at 5 percent, that is, at a blade loading of $\frac{k_{sa}}{\sigma} \cong 0.2$, on the basis of 0.7R blade chord. According to figure 14, the efficiency by best solidity of 67.8 percent for a rectangular blade rises to 72.2 percent on the untwisted blade and to 77.6 percent on the tapered blade with 6 percent negative twist. The taper factor was $p = -\frac{2}{3}$; on a blade continuing to rotor center the chord of the innermost blade element to the theoretical chord (rounding off disregarded) at the blade tip the ratio would be as 3:1. This 6° twisted blade approximately corresponds to the blade form in modern designs.

To sum up, it may be stated that as regards hovering (without consideration to forward flight) a rotor of light blade loading with low tip speeds is propitious. A suitable blade loading is $k_{sa}/\sigma \cong 0.2$. With a twisted tapered blade, the efficiency can be improved by about 15 percent over a normal rectangular blade, which is about equivalent to a 10-percent lift increase by equal power input.

In the following, the optimum solidity is briefly discussed which, mathematically, does not become evident with the assumption $B = 0.98 = \text{constant}$. Plotting the η values of figure 12 for the best blade loading $\frac{k_{sa}}{\sigma} = 0.2$ at the different thrust coefficients k_{sa} against the solidity (fig. 16) manifests a steady, slight rise in static-thrust coefficient with the solidity, which is not in accord with the facts.

Expressing the circulation decrease at the blade, conformable to Prandtl (reference 2)* with

$$B = 1 - \frac{\sqrt{k_{sa}}}{z} \qquad (83)$$

gives the values shown in figure 15 in relation to k_{sa} for different blade numbers z and hence a maximum of the static-thrust efficiency, which is in accord with the tests at solidities of from 8 to 12 percent (fig. 16).

However, since the optimum is very weakly marked, a solidity of 6 percent is not likely to be exceeded because of the weight of the blades and their sagging on the stand. Even then it affords blades with sufficient static-thrust efficiency and adequate high speed.

Gliding Coefficient for Best Horizontal Flight

This implies the efficiency of the best possible horizontal flight; that is, the prediction of the normally attainable lowest gliding coefficient without regard to speed. We proceed from the coefficient of advance $\mu = 0.35$, that is, the value at which the best gliding coefficient may be expected, according to past information. The 280-kilometers-per-hour speed limitation connected with it, according to figure 11, is disregarded.

The solidity, in accord with modern designs, is put at $\sigma = 0.05$. This is the same value that gave the best static-thrust coefficient for $k_{sa} = 0.009$ in the hovering stage. The first task involves the determination of the best blade loading. Inasmuch as a change in blade loading at a given solidity is equivalent to a change in thrust coefficient, the coefficients of horizontal thrust and torque were computed for $k_{sa} = 0.005$, 0.0075, 0.010 (corresponding to a blade loading $k_{sa}/\sigma = 0.10$, 0.15, 0.20) and plotted against α (figs. 17 to 21), along with the blade angle of attack ϑ_0 necessary for each slope of the normal plane to produce the required thrust (lift).

---

*In equation (4), v is replaced by v_d, and v^2 in the denominator disregarded with respect to $R^2\omega^2$. With $\lambda_d = \sqrt{k_{sa}}/1.4$, it affords

$$a = 1 - B = \frac{2 \ln 2}{1.4\, z}\sqrt{k_{sa}}$$

$$B \cong 1 - \frac{\sqrt{k_{sa}}}{z}$$

Figures 17 to 19 show this result for a rotor with a rectangular blade of zero twist; and figures 20 and 21, for the best of the three explored blade loadings $k_{sa}/\sigma = 0.15$, based on a rectangular blade of 6° negative twist and a tapered blade $\left(p = -\frac{2}{3}\right)$ of zero twist.

The results were obtained in the following manner: λ_d is first obtained from the axial thrust equations (13) and (41) as functions of the blade loading and the blade angle of attack, respectively, and then written in the formulas for the torque and the normal thrust coefficients. With λ_d and k_{sa}, the related α value is afforded from equation (1), thus leaving the transformation of the coordinates to be effected. By this transition to the propeller - to the wind system, the calculation of k_{sh} (horizontal thrust) was made with $\cos \alpha = 1$, and the vertical put equal to the axial thrust (fig. 4). Since in the case of practical interest α_{max} reaches about 10° to 14°, this omission has no significance so far as the result is concerned. Breakaway of flow was accounted for by $k_{sa}/\sigma = 0.15$ with $b = 0.7$, and by $k_{sa}/\sigma = 0.20$ with $b = 0.98$.

Further evaluation of the thus-obtained data consists in the calculation of the gliding coefficient ϵ, according to

$$\epsilon = \frac{k_{sh} + f \lambda^2}{k_{sv}} + \frac{k_d}{\lambda k_{sv}} \qquad (84)$$

where $f \lambda^2$ allows for the effect of additional resistance, such as fuselage, landing gear, and so forth. The factor f characterizes the ratio of parasite drag of all nonlifting parts of rotating-wing aircraft to swept rotor-disk area. All mechanical efficiencies of energy transmission and propeller efficiency are disregarded in equation (84) because of their subordinate role at this point.

In Part I (T.M. No. 921) it was stated that the required lift by equal rotor speed can be attained by different flight attitudes. The two extreme cases are briefly reviewed:

Autogiro: Up to about 5° blade angle of attack and positive setting of the normal plane relative to the air stream, the rotor is driven by the relative wind. A regular tractor propeller serves for overcoming the total drag.

Helicopter: The normal plane of a power-driven rotor is tilted forward (negative α) until the rotor itself overcomes its own drag and that of the aircraft. The blade angles of attack must be increased to about 10° to 12°; a separate propeller is no longer required.

Figure 22 gives the efficiency of horizontal flight by 0.35 coefficient of advance for these two extreme cases, without allowing for additional drag. The curves show the reciprocal gliding coefficient of a rotor with rectangular blade of zero twist in relation to the blade loading. For appraisal of the effect of twist and taper, the points for a twisted, rectangular blade and a tapered blade of zero twist have been added for $k_{sa}/\sigma = 0.15$. The helicopter shows a temporary superiority over the autogiro for $f = 0$. But, since a practical appraisal of the different flight stages must take additive resistance into account also, this comparison will be referred to again, later.

The best gliding coefficients for the autogiro with simple - that is, rectangular blade of zero twist, lies at $k_{sa}/\sigma = 0.16$; and for the helicopter at 0.14. In other words, to maintain the best ϵ on changing from hovering (best value at $k_{sa}/\sigma = 0.20$) to forward flight, theoretically requires an increase in rpm which, according to figure 22, should amount to 12 percent for the autogiro and 20 percent for the helicopter.

This well-known displacement of best blade loading on autogiros is in accord with wind-tunnel test data. The extensive measurements by Wheatley (reference 3) and evaluated by Hohenemser (reference 4) give, for instance, the best gliding coefficients at $k_{sa}/\sigma = 0.15$ blade loading. Corresponding helicopter tests are lacking.

For appraisal of the absolute values of the theoretical maximum efficiency of the helicopter, various full-scale measurements, as reported by Cierva in a lecture before the Royal Aeronautical Society, on March 15, 1935 (reference 5) may be employed. According to this, Wheatley's experiments on U.S. autogiro rotors yielded gliding coefficients of from 1:8 to 1:10. These figures would agree with the present calculation, which gives 1:8.4 as best value for the rectangular blade. The tapered blade affords mathematically an improvement to about 1:9 - thus also falling into Wheatley's range of test values, which likewise include blade shapes differing from

the plain rectangular blade. It should be borne in mind that on the tapered blade, with the same comparative solidity $\sigma_{0.7}$, the decisive outer blade elements operate at a lower characteristic coefficient than on the rectangular blade. Since this fact had not been taken into account in the calculation, the improvement in theoretical gliding coefficient achieved here probably does not become completely manifest. Cierva quotes ϵ = 1:13 to 1:14 as optimum values obtained by himself. However, since neither these nor similar favorable gliding coefficients have ever been definitely obtained up to now - neither by full-scale nor on models - these figures seem a little too optimistic.

Obviously, the gliding coefficients usually obtained in model tests, with a maximum of about 1:6, are substantially more unfavorable and not summarily applicable to appraisals of optimum values obtainable at full scale. This is chiefly due to the small characteristic values and, in a lesser degree, to the additional losses usually caused by the disproportionate dampers, hinges, and so forth, which do not always lend themselves to satisfactory mathematical treatment.

The effect of twist was illustrated on a rectangular blade with negative twist ($\vartheta_1 = -6^\circ$) for $k_{sa}/\sigma = 0.15$. The gliding coefficient of the helicopter showed an improvement from 1:10.3 to 1:10.9. On the autogiro with opposed flow, this negative twist is detrimental because the normal plane for the windmill state must be set too steep as a result of the inferior autorotation ability.

The tapered blade affords an improvement on the autogiro as on the helicopter, with an absolute best value of ϵ = 1:11, computed on the basis of a blade taper of 3:1 $\left(p = -\frac{2}{3}\right)$. With concurrent blade twist, this value presumably can be raised to about 1:12 which, in the author's opinion, is probably the upper limit for the present.

The effect of additional resistances is illustrated in figure 23, where the reciprocal ϵ of a rotor is plotted against the performance factor υ (characterization of flight stage) for various parasite areas. The performance factor is defined as the ratio of rotor input power to total power. Given the ϵ of a rotating-wing aircraft, the performance factor υ can be computed according to

$$\nu = \frac{k_d}{\lambda \epsilon k_{sv}} \qquad (85)$$

Figure 23 also shows the different angles of attack of the normal plane necessary to overcome the resistances of the aircraft in the helicopter state. The chosen representation has the advantage of placing for α = constant all potential flight stages on one straight line, which passes through the zero point of the coordinates with the inclination $\lambda k_{sv}/k_d$. The curves for ϵ were based on parasite areas of $f = 0.003$ and $f = 0.006$. The last value corresponds, for present-day dimensions, to a normal rotating-wing aircraft of the type of the C 30. $f = 0.003$ represents a particularly clean aerodynamic design. On the autogiro ($\nu = 0$) the parasite areas lower the gliding coefficient from 1:8.4 to 1:6.0 and 1:4.6, respectively. In the pure helicopter state ($\nu = 1$), ϵ is raised from 1:10.3 to 1:6.9 and 1:5.1, respectively. The forward tilt of the normal plane must, as a result of the additional resistances, be increased from $\alpha = -6.3^\circ$ of the rotor windmill state to -9.5° and -12.7°, respectively.

While the helicopter is superior for $f = 0$, the best ϵ for $f = 0.006$ lies with the helicogyro. Hence the superiority of the helicopter diminishes with increasing parasite drag relative to the other flight stages.

In the foregoing investigations the efficiency of the rotor drive and of a regular propeller required on occasion (autogiro or helicogyro) is disregarded. Since the gear efficiency is ordinarily substantially higher than the propeller efficiency, the helicopter superiority computed here is even more in evidence. This agrees with the flight tests of Focke's combined helicopter-autogiro, which attained the greater horizontal speed in the helicopter state.

CONCLUDING REMARKS

The best static thrust coefficients are obtained by blade loadings of $k_{sa}/\sigma = 0.2$, according to the study of the hovering state, and this figure can be raised by about 15 percent by using a tapered blade.

On passing from hovering to horizontal flight, the best blade loading for the explored coefficient of advance of

0.35 shifts to $k_{sa}/\sigma = 0.16$ for the autogiro and to $k_{sa}/\sigma = 0.14$ for the helicopter, hence the rpm should be increased.

The absolute best ϵ is to be expected at speeds below 300 kilometers per hour. It should amount to about 1:12 for the rotor without additional resistances when using a blade which is favorable for hovering also. A comparison of the different flight states gives for $\mu = 0.35$ in agreement with flight tests, a superiority of the helicopter which, though it may not be generalized, makes it likely that the helicopter, because of its superior take-off and landing characteristics, will be successful in the near future.

Since additional resistances are more detrimental to the gliding coefficient of the helicopter than on the autogiro, the greatest value for the helicopter should be placed upon an aerodynamically favorable design of the whole aircraft.

Translation by J. Vanier,
National Advisory Committee
for Aeronautics.

REFERENCES

1. Stack, John, and von Doenhoff, Albert E.: Tests of 16 Related Airfoils at High Speeds. T.R. No. 492, NACA, 1934.

2. Prandtl, L., and Betz, A.: Vier Abhandlungen zur Hydrodynamik und Aerodynamik, Nachsatz Prandtl zu Betz, Schraubenpropeller mit geringstem Energieverlust. Kaiser Wilhelm Instituts für Strömungsforschung, Göttingen, 1927.

3. Wheatley, John B., and Bioletti, Carlton: Wind-Tunnel Tests of 10-Foot-Diameter Autogiro Rotors. T.R. No. 552, NACA, 1936.

4. Hohenemser, K.: Performance of Rotating-Wing Aircraft. T.M. No. 871, NACA, 1938.

5. Cierva, Juan de la: New Developments of the Autogiro. Paper read before Society, March 15, 1935. Jour. R.A.S., Dec. 1935, pp. 1125-37.

XII. Tables

Table 1 (Fig. 12)

	k_{sa}/σ	$10^3\,k_d$	η %		k_{sa}/σ	$10^3\,k_d$	η %
$k_{sa} = 0{,}003$	0,06	0,213	38,5	$k_{sa} = 0{,}006$	0,06	0,495	46,9
	0,09	0,173	47,5		0,09	0,418	55,5
	0,12	0,156	52,6		0,12	0,384	60,4
	0,18	0,147	55,8		0,18	0,364	63,8
	0,24	0,148	55,5		0,24	0,368	63,0
	0,30	0,154	53,3		0,30	0,380	61,0

Table 1 (continued)

	k_{sa}/σ	$10^3\,k_d$	η %		k_{sa}/σ	$10^3\,k_d$	η %
$k_{sa} = 0{,}009$	0,06	0,825	51,7	$k_{sa} = 0{,}012$	0,06	1,195	55,0
	0,09	0,708	60,2		0,09	1,028	63,8
	0,12	0,659	64,7		0,12	0,970	67,7
	0,18	0,630	67,8		0,18	0,932	70,4
	0,24	0,635	67,2		0,24	0,938	70,0
	0,30	0,652	65,4		0,30	0,961	68,4

Table 2 (Fig 13)

k_{sa}	ϑ_1	p	σ	$10^3\,k_d$	η %
0,009	0	0	0,02	0,721	59,2
			0,03	0,651	65,5
			0,04	0,631	67,6
			0,05	0,628	67,8
			0,06	0,637	67,0
			0,07	0,650	65,6
			0,08	0,668	63,8
			0,10	0,708	60,2
			0,12	0,754	56,6
0,009	-6^0	0	0,02	0,701	60,9
			0,03	0,627	68,0
			0,04	0,603	70,8
			0,05	0,598	71,3
			0,06	0,604	70,6
			0,07	0,614	69,5
			0,08	0,628	68,0
			0,10	0,663	64,5
			0,12	0,702	60,8
0,009	-12^0	0	0,02	0,683	62,5
			0,03	0,606	70,5
			0,04	0,579	73,5
			0,05	0,571	74,7
			0,06	0,573	74,5
			0,07	0,581	73,5
			0,08	0,591	72,3
			0,10	0,620	68,8
			0,12	0,652	65,5

Table 3 (Fig. 14)

k_{sa}	ϑ_1	p	$\sigma_{0,7}$	$10^3\,k_d$	η %
0,009	0	0	0,02	0,721	59,2
			0,03	0,651	65,5
			0,04	0,631	67,6
			0,05	0,628	67,8
			0,06	0,637	67,0
			0,07	0,650	65,6
			0,08	0,668	63,8
			0,10	0,708	60,2
			0,12	0,754	56,6
0,009	0	$-2/3$	0,02	0,685	62,2
			0,03	0,616	69,3
			0,04	0,593	71,8
			0,05	0,590	72,2
			0,06	0,595	71,6
			0,07	0,607	70,2
			0,08	0,621	68,7
			0,10	0,656	65,0
			0,12	0,697	61,1
0,009	-6^0	$-2/3$	0,02	0,659	64,8
			0,03	0,586	72,8
			0,04	0,559	76,3
			0,05	0,551	77,4
			0,06	0,553	77,2
			0,07	0,560	76,2
			0,08	0,570	74,9
			0,10	0,597	71,5
			0,12	0,628	67,9

Table 4.

	ϑ_0	λ_d	α^0	$10^3 \cdot k_d$	$10^3 \cdot k_{sn}$	$10^3 \cdot k_{sh}$	
$k_{sa}/\sigma = 0{,}15,\ \vartheta_1 = 0^0,\ p = 0$	2	+0,0269	+5,3	−0,089	+0,534	+1,255	Fig. 18
	5	−0,0111	−0,9	+0,081	+0,725	+0,602	
	8	−0,0488	−7,1	+0,291	+0,854	−0,086	
	11	−0,0868	−13,1	+0,543	+0,920	−0,782	
	14	−0,1246	−18,9	+0,837	+0,923	−1,524	
$k_{sa}/\sigma = 0{,}15,\ \vartheta_1 = -6^0,\ p = 0$	6	+0,0290	+5,6	−0,072	+0,456	+1,191	Fig. 20
	9	−0,0092	−0,6	+0,080	+0,668	+0,586	
	12	−0,0470	−6,8	+0,258	+0,818	−0,074	
	15	−0,0852	−12,8	+0,455	+0,906	−0,754	
	18	−0,1232	−19,4	+0,703	+0,931	−1,569	
$k_{sa}/\sigma_{0,7} = 0{,}15,\ \vartheta_1 = 0^0,\ p = -2/3$	2	+0,024	+4,8	−0,032	+0,325	+0,955	Fig. 21
	4	+0,001	+1,0	+0,062	+0,504	+0,641	
	6	−0,022	−2,7	+0,159	+0,645	+0,289	
	8	−0,045	−6,5	+0,271	+0,750	−0,105	
	10	−0,068	−10,1	+0,401	+0,818	−0,502	
	12	−0,091	−13,8	+0,557	+0,849	−0,931	
	14	−0,114	−17,3	+0,711	+0,844	−1,391	
$k_{sa}/\sigma = 0{,}10,\ \vartheta_1 = 0^0,\ p = 0$	−1	+0,0474	+8,3	−0,042	+0,156	+0,886	Fig. 17
	1	+0,0220	+4,2	+0,015	+0,274	+0,639	
	3	−0,0032	+0,1	+0,085	+0,364	+0,369	
	5	−0,0288	−4,1	+0,166	+0,426	+0,066	
	7	−0,0538	−8,2	+0,264	+0,461	−0,259	
	9	−0,0791	−12,2	+0,375	+0,468	−0,585	
	11	−0,1043	−16,1	+0,497	+0,447	−0,938	
$k_{sa}/\sigma = 0{,}20,\ \vartheta_1 = 0^0,\ p = 0$	4	+0,0188	+4,3	−0,139	+1,000	+1,742	Fig. 19
	6	−0,0064	+0,1	+0,018	+1,163	+1,184	
	8	−0,0318	−4,1	+0,193	+1,299	+0,592	
	10	−0,0571	−8,1	+0,387	+1,409	−0,020	
	12	−0,0826	−12,1	+0,600	+1,491	−0,600	
	14	−0,1076	−16,0	+0,831	+1,545	−1,215	

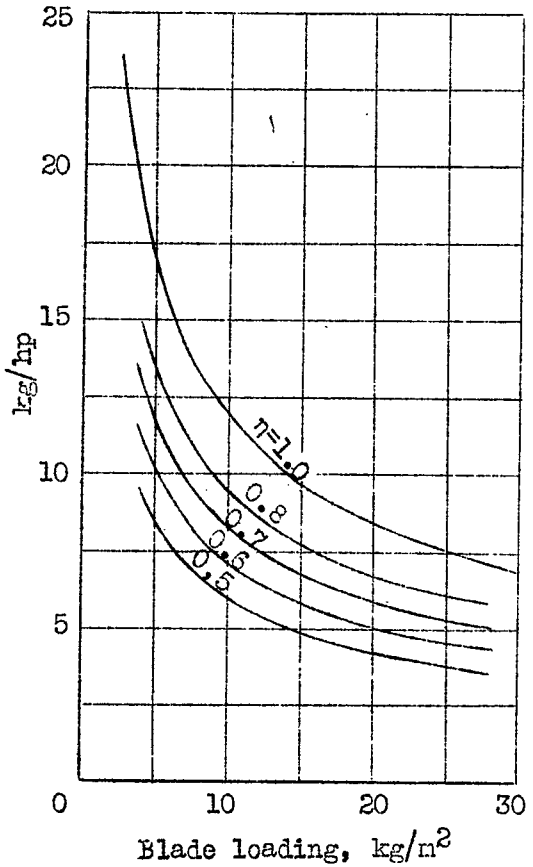

Figure 8.- Thrust in hovering state plotted against blade loading.

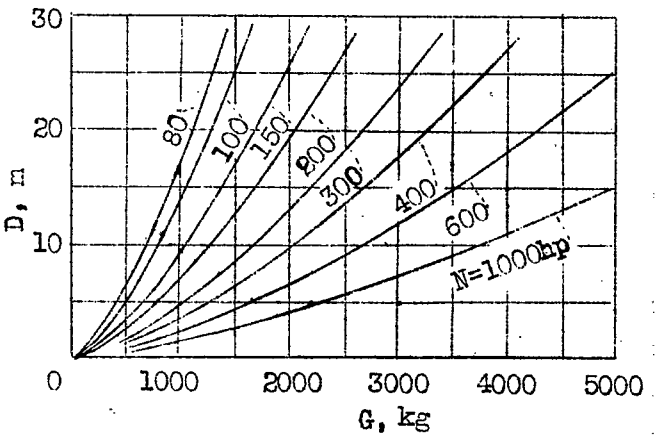

Figure 9.- Minimum diameter of swept rotor disk for hovering.

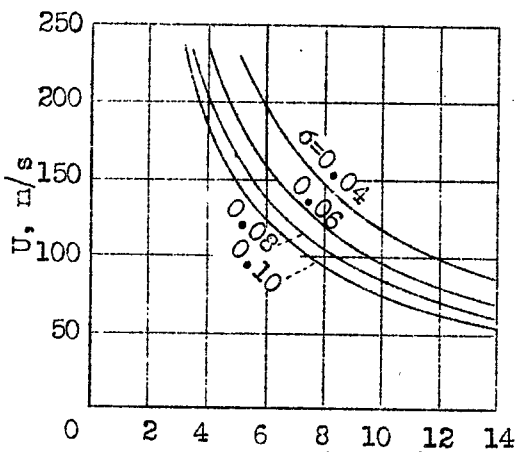

Figure 10.- Best tip speed for hovering.

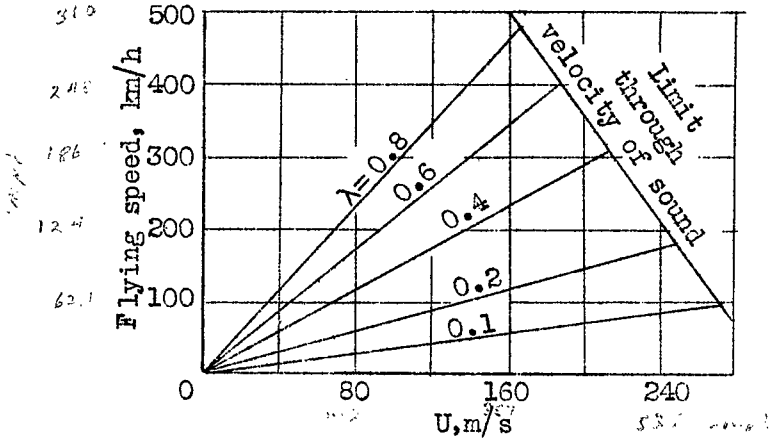

Figure 11.- Speed limit at highest permissible Mach number of 0.9.

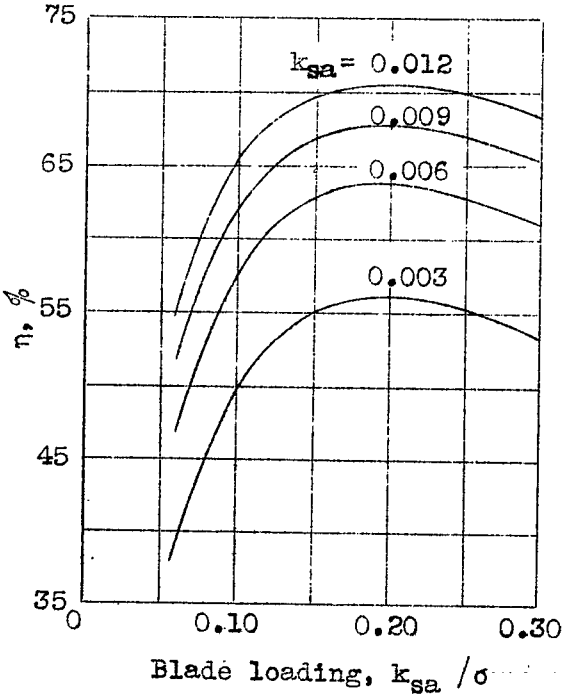

Figure 12.- Static thrust coefficient of plain rectangular blade.

Figure 13.

Static thrust coefficient of rectangular blade improved by twist (k_{sa} = 0.009).

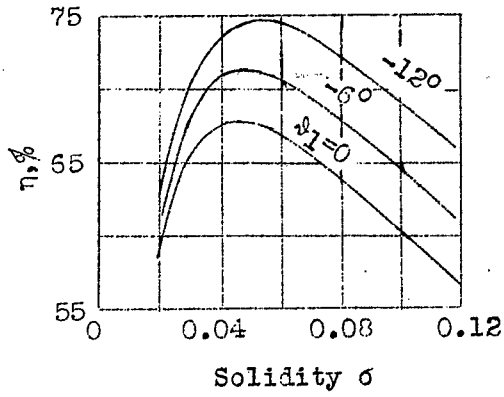

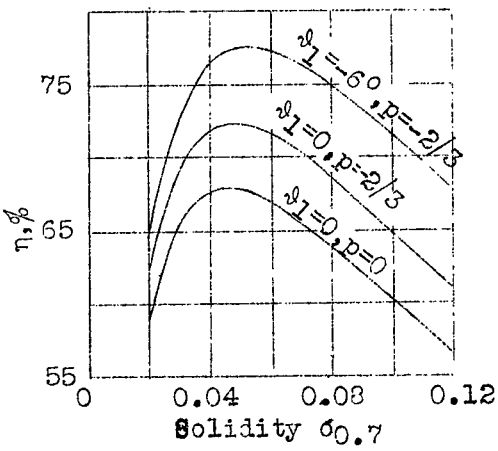

Figure 14.

Static thrust coefficient improved by changing from a simple rectangular blade to a plain and a twisted tapered blade (k_{sa} = 0.009).

Figure 16.

Static thrust coefficient of rectangular blade with zero twist by best blade loading $\left(\frac{k_{sa}}{\sigma} = 0.2\right)$ in relation to solidity.

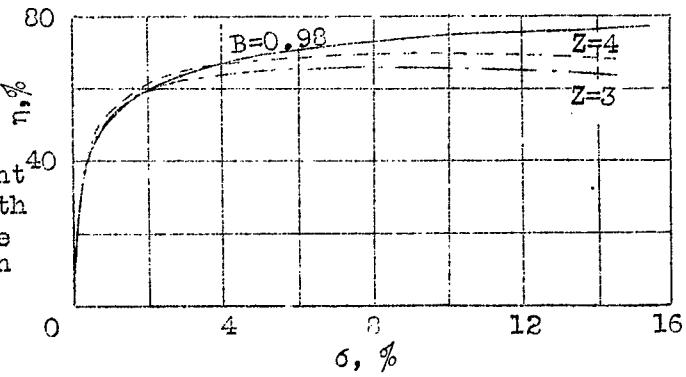

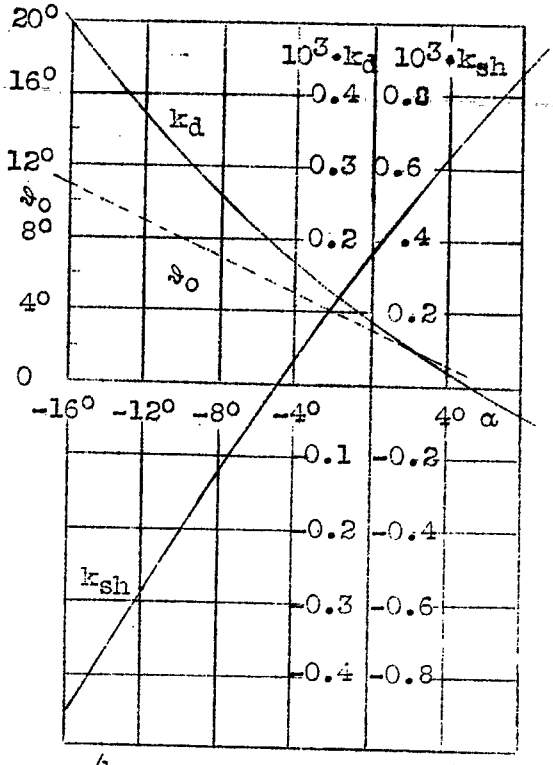

Figure 17.- Plain rectangular blade (no twist).

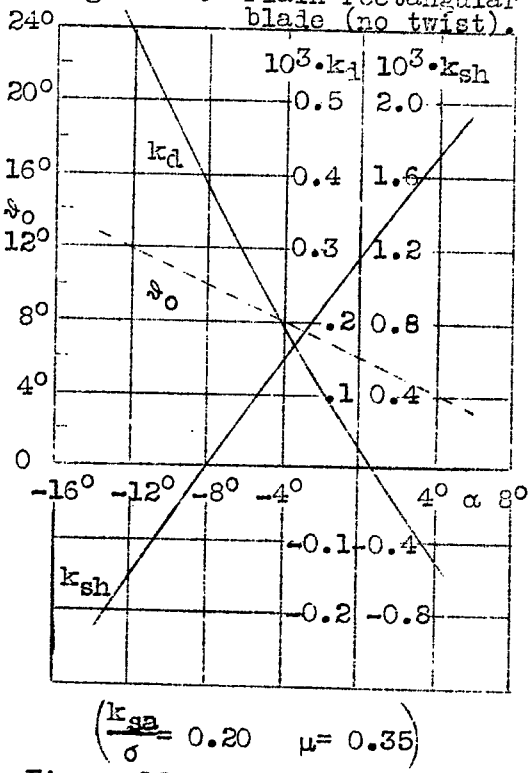

Figure 19.- Plain rectangular blade (no twist).

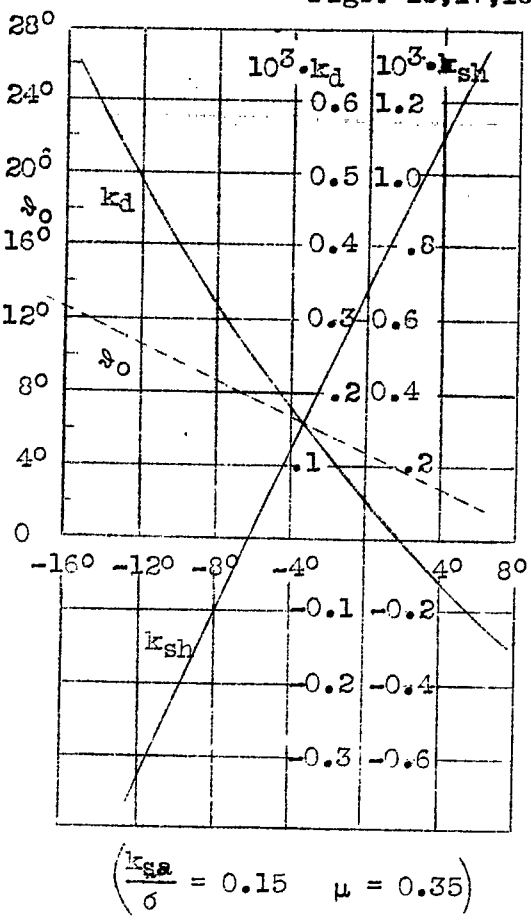

Figure 18.- Plain rectangular blade (no twist).

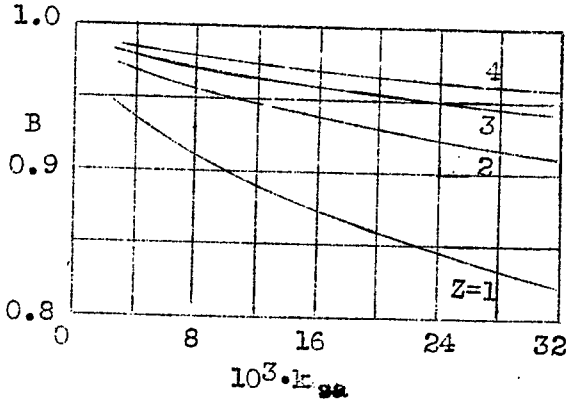

Figure 15.- Effect of finite blade number and rotor loading on the thrust reduction factor B.

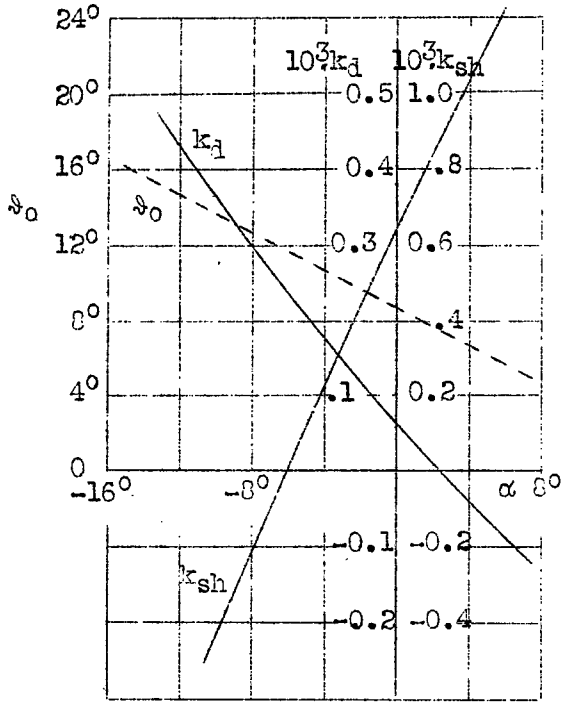

$\frac{k_{sa}}{\sigma}$=0.15 μ=0.35 ϑ_1=-6°

Figure 20.- Twisted rectangular blade.

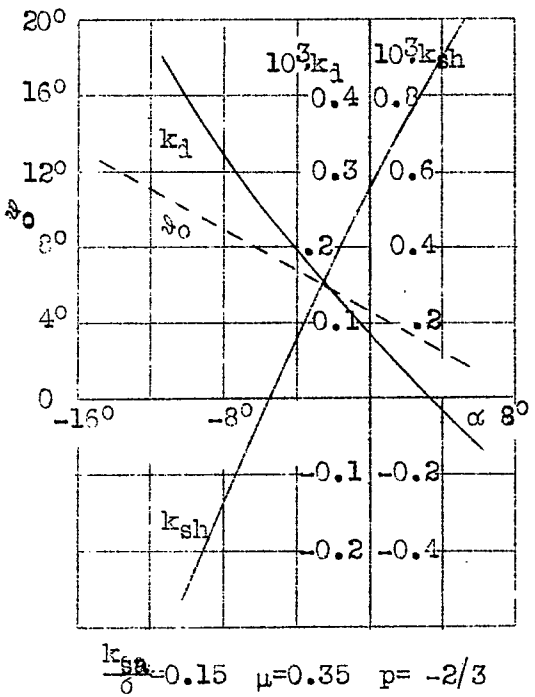

$\frac{k_{sa}}{\sigma}$=0.15 μ=0.35 p= -2/3

Figure 21.- Tapered blade, zero twist.

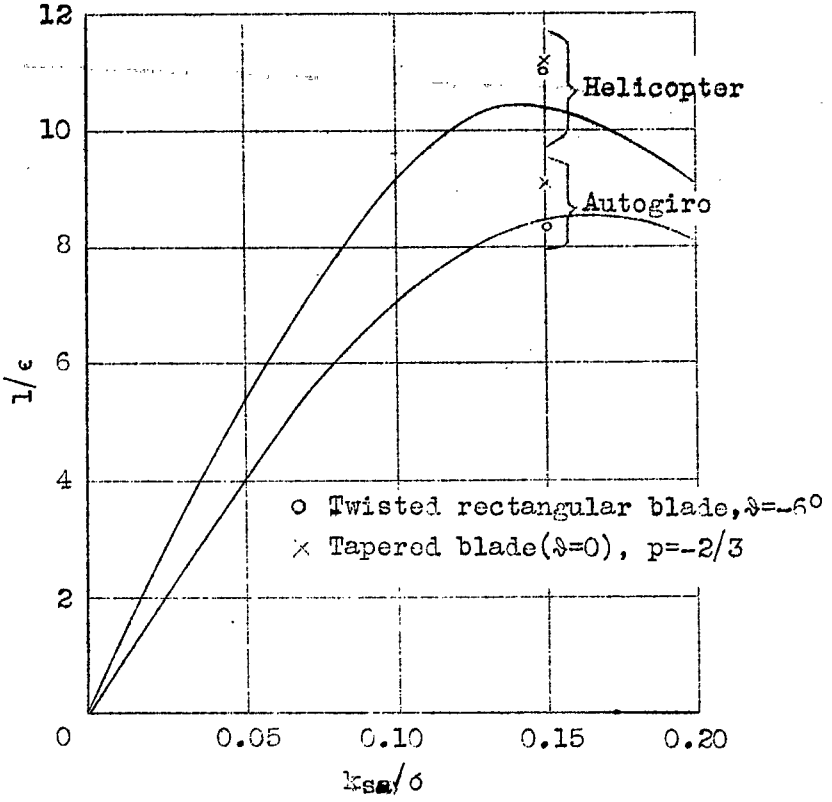

Figure 22.- Efficiency of rotor running by itself (f=0) in autogiro and helicopter state.
(Rectangular blade, μ= 0.35, zero twist)

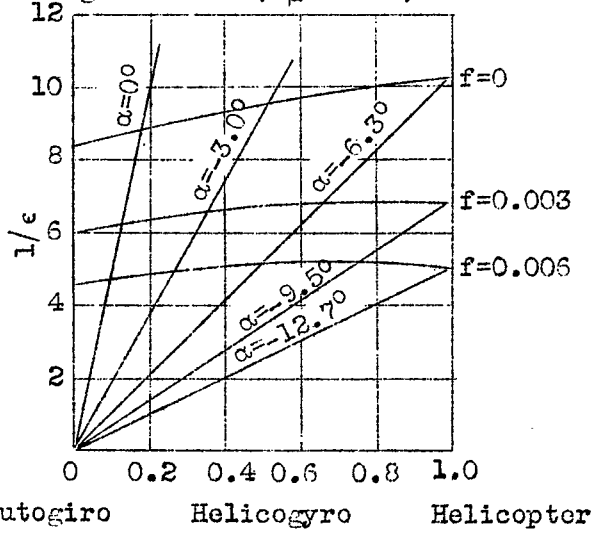

Figure 23.- Effect of equivalent parasite area by μ= 0.35.
$\left[\text{Rectangular blade}, \frac{k_{sa}}{\sigma} = 0.15, (\phi=0)\right]$